Optimized Pi Controller With Hybrid Sealion-Dragon Fly Algorithm For Grid-Tied PV System

Thomas Thangam[1*], R.Hemalatha[2], M. Murali [3], V. Joshi Manohar [4]

Abstract: The significance of solar energy in recent days has evidently increased with multiple benefits, because of which it is preferred in various applications of both rural and urban places. In this work, a SEPIC converter based 1Φ grid tied PV system with a hybrid sea lion and dragonfly algorithm is employed. Generally the output of PV is obtained as low, to maximize the voltage level and to terminate the voltage fluctuations, the SEPIC converter is propounded in this work since it owns the capability of effectual voltage gain ratio. A closed loop control with PI controller has been implemented to maintain DC-link voltage as constant and a hybrid sea lion and dragonfly algorithm is introduced to tune parameters of PI controller. Then the obtained value is given to the grid through a 1Φ VSI, which has assisted in converting the DC into AC. The PI controller has aided in generating the mandatory gating pulses of the VSI; the actual and reference powers are analogised, through which the grid synchronization and reactive power compensation have been magnificently achieved. The entire process has been validated through the MATLAB Simulink.

Key Words: *Hybrid sea lion and dragonfly algorithm, SEPIC converter, PV system, grid synchronization, PI controller, MATLAB.*

1. Introduction

In the present scenario, the generation of PV has occupied a prominent place in multiple sectors and its contribution in power electrical applications is remarkably high since it is wrapped with bunch of benefits like stable structure, simple implementation, less maintenance, extreme storage capacity and affordable price. It is highly feasible to install this PV system in both the urban and rural areas and for this reason, many organizations including governmental and non-governmental concerns have encouraged the implementation of PV system, through which the constant power flow is achieved without any hurdles [1]. Through the utilization of PV in a wider range, the pollution free environment is made possible since the risk factors like CO_2 emission and Global warming are minimized with the usage of renewable energy resources like solar and wind energies [2]. This PV system is preferably used as two different modes called standalone and grid tied systems, among which the standalone system requires adequate batteries with high power storage capacity, which demand high cost of implementation whereas there is no necessities of

batteries in grid tied system; thus the grid tied PV system is considerable with economical friendliness [3]. Because of these desirable privileges, this system has been attracted by many researchers, who have done various investigations on this PV system and introduced multiple novel ideas regarding the implementation of grid connected PV system [4]. In spite of these remarkable benefits, the source voltage of PV is too low, which is not capable enough to meet the reference voltage, hence the generated voltage of PV has to be maximized in an efficient way. A transformer is used in the early days for the voltage compensation yet that has not succeeded since the bulky nature of the transformer has increased the volume of the system, which causes the minimization of overall performance and efficacy of the system. Thus to improve the voltage gain, a DC-DC converter is developed, which has eradicated the usage of transformers and enhanced the reliability of the system [5].

Stepping up the voltage with the assistance of DC-DC converters is the essential process, which results in effectually utilizing the PV source and different converters have been used in the past days for doing so

---

[1] *Lecturer, Department of Process Engineering, International Maritime College Oman*
[2] *Assistant Professor, Department of Electrical and Electronics Engineering, Saveetha Engineering College.*
[3] *Associate Professor in the Department of Electrical Engineering at Medi-Caps University, Indore, MP, India.*
[4] *Head of Department & Professor at Presidency University, Itgalpur, India.*
* *Corresponding Author Email: tjthomasthangam@gmail.com*

[6,7]. In order to escalate the voltage efficiency, the boost converters are utilized in the initial days but the attained voltage of these converters are in the fluctuated state and have not met the necessity of grid voltage [8, 9]. Hence a buck-boost converter is employed, which is capable of operating in both the buck and boost mode to sustain the voltage gain of the system [10]. Though it is beneficial, this converter has certain limitations in boosting up the voltage ratio, which have been eradicated with the utilization of CUK converters. These converters have elevated the range of obtained values but the attained voltage is not sufficient for power generation of PV [11]. Thus a SEPIC converter is introduced in this present work to overcome all the above mentioned issues.

The power generation of this system is enhanced by tracking the maximum power, which has been acquired by using the traditional MPPT techniques like P&O and Incremental Conductance but they are not highly effectual in all situations [12, 13]. Therefore, a closed loop control system with PI controller has been employed to escalate the efficacy and reliability of maximum power extraction since it is capable enough to extricate the maximum power [14, 15]. The gain values of PI controller have been attained through the implementation of several algorithms, among which the trial & error is conventionally used but it delivers poor performance hence it is overcome with the implementation of Fuzzy logic control, which shows better performance with extreme time consumption [16]. Thus to elevate the performance of the PI with precise time, the approaches like Genetic Algorithm (GA) and Particle Swam Optimization (PSO) have been employed but the attained values of these methods are not well-tuned since it delivers oscillation in producing optimal values [17, 18]. Hence, to mitigate these issues, Grey Wolf Optimization is introduced, which has remarkably overcome these problems [19, 20] yet this is not applicable in all circumstances. Thus a hybrid algorithm is employed in this present study to elevate the performance of PI controller. The attained DC voltage is not directly fed to the grid and it has to be converted into AC, for which Voltage source inverter is implemented [21].

In the present study, SEPIC converter is utilized to acquire essential voltage and converter is regulated through hybrid sea lion and dragonfly algorithm. The grid synchronization is attained with the aid of PI controller. The remaining parts of this study envelopes the subsequent elements like working of proposed system, modeling of PV module, modeling of SEPIC converter, closed loop control with PI controller using hybrid sea lion and dragonfly algorithm, modeling of 1Φ VSI and Grid.

2. Proposed Control Scheme

The proposed control strategy for PV linked grid with SEPIC converter, hybrid sea lion and dragon fly algorithm is represented in Fig 1. The PV system used in this control scheme generally provides low DC voltage due to its solar irradiation.
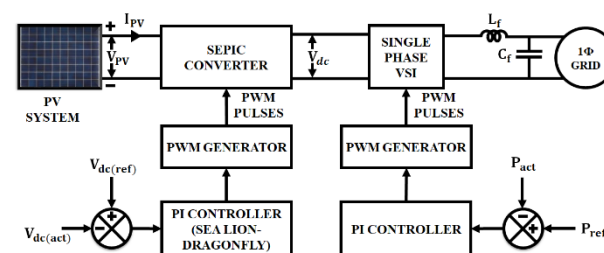

Fig. 1. Proposed Control strategy

In this control scheme, the SEPIC converter is proposed to boost up PV module's low DC voltage into high DC voltage and also it reduces the ripples present in PV voltage. By using a Hybrid sea lion and dragon fly based PI algorithm, the SEPIC converter's gating pulses are controlled by means of PI controller and the parameters of PI are adjusted with the help of proposed algorithm and so the output of DC-link voltage is retained to be as constant. To synchronize the PV with the utility grid, the attained DC voltage is then converted to AC and the conversion of DC to AC takes place by using 1Φ VSI. The gating sequence for the inverter is controlled with the aid of PI controller and so the grid synchronization and reactive power compensation is achieved by analogizing P_{act} with P_{ref} values.

3. Modeling Of The Proposed Control Scheme

3.1 Modeling of PV system

PV system transforms the solar energy into direct current by using photovoltaic semiconducting materials. To generate required solar energy, a photovoltaic system uses solar panels which are made up of a variety of solar cells. Irradiance and temperature are the important factors to consider when modelling this system. The output voltage from a PV system is oscillating due to changes in irradiance and temperature. In this paper, a high gain SEPIC converter is employed to minimize the oscillation and maximize the output power from solar in an efficient way. The circuit layout for PV module is illustrated in Fig 2.
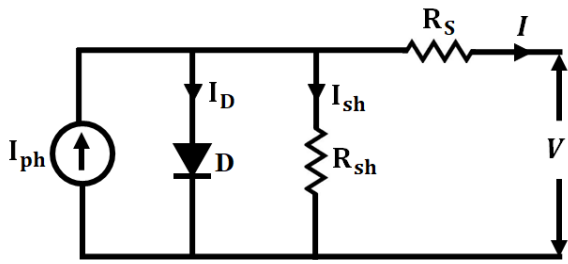
Fig. 2. Circuit layout of PV module

The current flow through PV module is expressed as,

$$I = I_{ph} - I_o \left[e^{\frac{(V+R_sI)}{V_k\alpha}} - 1 \right] - \frac{V+IR_s}{R_{sh}} \qquad (1)$$

Where the SC PV current is denoted as I_o, the maximum thermal voltage is denoted as V_k, the diode ideality constant is denoted as α, input photo current is denoted as I_{ph}, diode current is denoted as I_d, the series and shunt resistances are represented as R_s and R_{sh}, the output PV current is denoted as I and the PV voltage is denoted as V. The output obtained from PV is low voltage, which is then fed to SEPIC converter.

3.2 Modelling of SEPIC converter

The SEPIC converter used in this proposed work in order to boost the PV modules low voltage DC into high DC voltage and this converter comprises PV voltage V_{PV}, switch S, inductances L_1, L_2, capacitances C_{in}, C_1, C_2, diode D and resistive load R_L. The operating modes and the design analysis of SEPIC converter are explained below and circuit layout is illustrated in Fig 3.
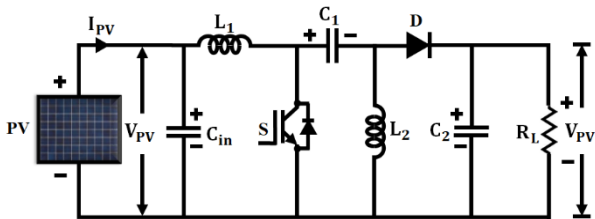

Fig. 3. Circuit layout of SEPIC converter

SEPIC is a kind of DC-DC converter, which permits output potential to be greater than, less than or equal to the input potential and IGBT used in this circuit controls SEPIC converter's output voltage. It is similar to a traditional buck-boost converter and the benefit of using this converter are it gives a non-inverted output due to the energy coupling from the input to the output through a series capacitor.

Mode 1

In mode 1, switch S is in ON state, inductance L_1 is charged by the PV voltage V_{PV} and the capacitance C_1, the capacitance C_2 energise the inductance L_2. The diode D is reverse biased and the output voltage is controlled by the capacitance C_2 which supplies power to the

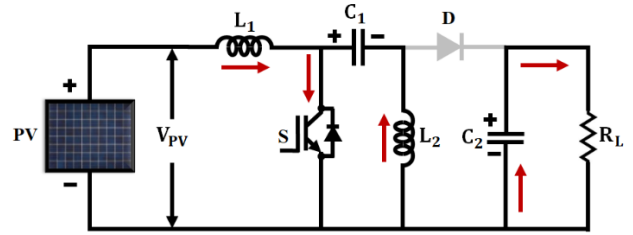resistive load R_L. The circuit layout of mode 1 is illustrated in Fig 4.

Fig. 4. Circuit layout of mode 1

The voltage across the inductance L_1 is expressed as,

$$V_{PV} = V_{L_1(ON)} \qquad (2)$$

$$V_{L_1} = L\frac{di}{dt} \qquad (3)$$

$$\frac{\Delta I_{L_1}}{T_{ON}} = \frac{V_{L_1(ON)}}{L_1} \qquad (4)$$

Mode 2

In mode 2, switch S is in OFF state and diode D is forward biased. The inductance L_1 discharges through coupling capacitor, whereas the power in the inductance L_2 discharges via capacitor output and also sent it to the resistive load R_L. The circuit layout of mode 2 is illustrated in Fig 5.
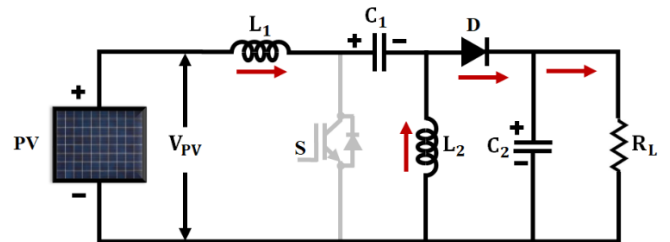

Fig. 5. Circuit layout of mode 2

The voltage across the inductance L_1 is expressed as,

$$V_{L_1(OFF)} = V_{C_1} + V_{OUT} - V_{PV} \qquad (5)$$

$$L\frac{di}{dt} = V_{C_1} + V_{OUT} - V_{PV} \qquad (6)$$

$$\frac{\Delta I_{L_1(OFF)}}{T_{OFF}} = \frac{V_{C_1} + V_{OUT} - V_{PV}}{L_1} \qquad (7)$$

The output potential of SEPIC converter is expressed as,

$$V_o = \frac{D * V_{PV}}{1-D} \qquad (8)$$

From this equation, the duty cycle is computed easily, thus by using this converter it stepped-up the PV module's low voltage to a higher value and also it reduces the ripples which occur in DC-link voltage.

3.3 Closed loop control with PI controller using sea lion and dragonfly algorithm

The SEPIC converter is managed by a closed loop control using PI controller, and PI parameters are adjusted by a proposed hybrid sea lion and dragonfly algorithm. In PI controller, the maximum peak over

shoot issues and steady state error occurs, the above mentioned issues are overcome by tuning the PI controller with hybrid sea lion and dragonfly algorithm. A PI controller gains such as proportional gain K_p and integral gain K_i is expressed as,

$$C(s) = K_p + \frac{K_i}{s} \qquad (9)$$

The parameters of PI controller such as K_p and K_i define the system's optimal operation, so these values are to be optimized.

Sea lion (SL) optimization algorithm

SL algorithm is an optimization algorithm which is based on actions of sea lions while hunting, exploration (searching) and exploitation (attacking) are the two phases of this algorithm. Sea lions has some interesting characteristics such as quick movement, sharp vision, and superior hunting ability. The major stages of sea lion hunting activity are shown below,

- Using their whiskers, they track and chase the prey.

- Pursing and encircling the prey, calling other members who had joined their subgroup.

- Attacking the prey.

Sea lion move in the following manner as they approach their intended prey:

$$\overrightarrow{J(t+1)} = \overrightarrow{M(t)} - \overrightarrow{Dis}.\vec{H} \qquad (10)$$

Where $\vec{J}(t)$ denotes position vector of sea lion, $\vec{M}(t)$ denotes position vector of target prey and $\overrightarrow{Dis}$ denotes distance between sea lion and target prey.

Distance between sea lion and target prey which is expressed as,

$$\overrightarrow{Dis} = \left| 2\vec{B}.\overrightarrow{J_{rand}(t)} - \overrightarrow{J(t)} \right| \qquad (11)$$

Where $\vec{B}$ denotes the random vector.

Because sea lions can live on land and in the water, they are classified as amphibians. The vocal behavior of sea lions is in such a way its sound travels four times quicker in water than in land. Once sea lion identify its prey, it call other sea lions for attacking the prey. The sea lion which identifies the prey is termed as the leader and its vocalization behavior is mathematically expressed as,

$$\overrightarrow{SP_{leader}} = \left| (\overrightarrow{V_1}(1 + \overrightarrow{V_2}))/\overrightarrow{V_2} \right| \qquad (12)$$

$$\overrightarrow{V_1} = \sin\theta \ ; \ \overrightarrow{V_2} = \sin\phi \qquad (13)$$

Here the sea lion's speed of sound is denoted as $\overrightarrow{SP_{leader}}$, sea lions speed of sound in water and air are denoted as $\overrightarrow{V_1}$ and $\overrightarrow{V_2}$ respectively.

During exploitation, sea lions identify prey and encircles the prey. The leader which is informs other sea lions is termed as the search agent, and prey is termed as the current best solution. The encircling behavior is mathematically expressed as,

$$\overrightarrow{J(t+1)} = |\vec{M}(t) - \vec{J}(t)|.cos(2\pi l) + \vec{M}(t) \qquad (14)$$

Where distance among optimum solution and search agent is denoted by $|\vec{M}(t) - \vec{J}(t)|$, $|\ |$ denotes absolute value and l denotes random number between $-1 \ to \ 1$. As hunting behaviour of sea lion is in a circular fashion, it is expressed mathematically as $cos(2\pi l)$.

As per the equation (15), in the exploration process, search agent's location is rationalized in accordance with randomly selected sea lion which and expressed as,

$$\overrightarrow{J(t+1)} = \vec{J}_{rnd}(t) - \overrightarrow{Dis}.\vec{H} \qquad (15)$$

Where $\vec{J}_{rnd}$ denotes arbitrary search agent, $\vec{H}$ denotes constraint which is steadily decreased from $2 \ to \ 0$.

Dragonfly algorithm

Exploitation and exploration are two stages that closely resemble swarm behaviour, and the DA algorithm is based on the behaviour of static and dynamic swarming inspiration.

As per equation (14), the formula for separation which is expressed as,

$$D_i = \sum_{l=1}^{M} J - J_l \qquad (14)$$

Where J_l denotes the lth location of close to individual, J denotes the location of current individual and M denotes the close to individual's count.

As per equation (15), the formula for alignment which is expressed as,

$$Z_i = \frac{\sum_{l=1}^{M_b} Q_l}{M_b} \qquad (15)$$

$$A_i = \frac{\sum_{l=1}^{M_b} J_l}{M_b} - J \qquad (16)$$

$$F_i = J^+ - J \qquad (17)$$

As per equation (18), the distraction from the enemy is specified which is expressed as,

$$E_i = J^- + J \qquad (18)$$

Where J^- denotes the location of enemy, the vectors such as step (ΔJ) and location (J) are calculated for updating the location of dragonfly.

As per equation (19), the distance to food (DF) is computed that depends upon the Euclidean distance (EU) which is expressed as,

$$DF = EU(J - J^+) \qquad (19)$$

As per equation (20), the variables of random ra is determined which is expressed as,

$$ra = \frac{ub+lb}{4} + \left((ub - lb) \times \left(\frac{it}{\max it} \right) \times 2 \right) \quad (20)$$

Where ub and lb denotes the upper and lower bounds.

As per equation (21), the updation takes place which is expressed as,

$$\Delta J(it + 1) = w\Delta J(it) + rZ_i + rA_i + rD_i \quad (21)$$

Where D_i denotes the separation of ith individual, A_i denotes the cohesion of ith individual, Z_i denotes alignment and w denotes inertia weight.

As per equation (22), the updation based on levy takes place which is expressed as,

$$J(it + 1) = J(it) + Levy(z) \times J(it) \quad (22)$$

Where z denotes the dimension and it denotes current iteration.

As per equation (23), the levy flight is computed which is expressed as,

$$Levy(x) = 0.01 \times \frac{r_1 \times \delta}{|r_2|^{\frac{1}{\eta}}} \quad (23)$$

$$\delta = \left(\frac{\Gamma(1+\eta) \times \sin\left(\frac{\pi\eta}{2}\right)}{\Gamma\frac{(1+\eta)}{2} \times \eta \times 2^{\left(\frac{\eta-1}{2}\right)}} \right)^{\frac{1}{\beta}} \quad (24)$$

As per equation (25), the step vectors direction of dragonfly movement is shown which is expressed as,

$$\Delta J(it + 1) = (qD_i + aZ_i + cA_i + fF_i + bE_i) + w\Delta J(it) (25)$$

Where weight of separation is denoted as q, weight of alignment is denoted as a, weight of cohesion is denoted as c, food factor is denoted as f, food resource of ith individual is denoted as F_i, enemy factor is denoted as b, and location of enemy with i^{th} individual is denoted as E_i.

Hybrid SL-DF Algorithm

The hybridized dragonfly and sea lion approach has wide range of applications because it improves performance of PI controller by tuning the parameters in an appropriate way. Set up N dragonflies as search agents and assess the fitness function as well as location of food source and enemy. Update location and fitness value of the food source with the outstanding fitness value of the search agent, while the enemy's location and fitness value is updated with the worst fitness value. Update the position and velocity vector if the number of neighbour search agents are less than or equal to 1. The new positions are adjusted based on the boundaries of K_p and K_i. Select 10 best particles for SL algorithm only after attaining maximum iteration or else repeat the same procedure.

The exploitation phase and exploration phase are the two stages of the sea lion algorithm. The sea lions upgrade their positions depends on best search element during exploitation period. During the exploration period, the search agents update their positions based on a randomly chosen sea lion. Over course of iterations, for the exploration and exploitation stages, parameter C is decreased from 2 to 0. When the value of |C| exceeds 1, it means that the search agent was chosen at random. When the value |**C**| is less than 1 then it indicates that search agents are updating their position. Finally, the SL algorithm is terminated when an ending criterion is met.
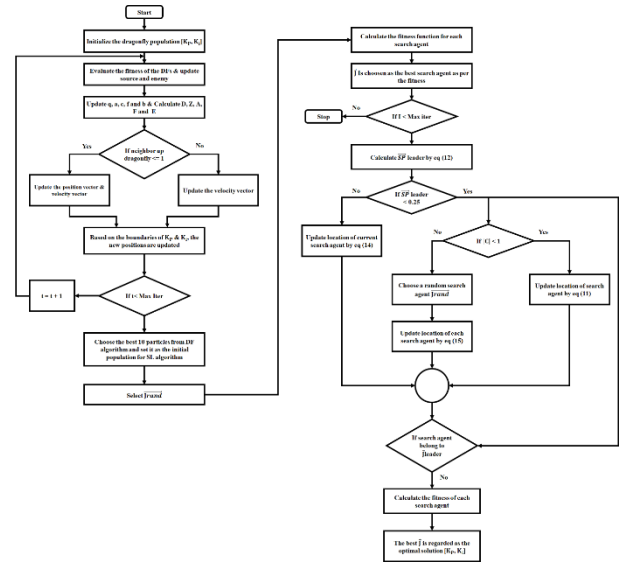

Fig. 6. Flowchart of hybridized DF-SL algorithm

Modelling of 1Φ VSI and Grid

With the help of a SEPIC converter, the input voltage from the PV is increased, and the SEPIC converter's output, a DC-link voltage, is kept constant by a PI algorithm based on a hybrid of the sea lion and the dragon fly. By employing 1 VSI to convert the obtained voltage into AC in order to synchronise with the grid, DC is transformed to AC. The VSI used in this system is full bridge VSI, this inverter produces output power double as that of half bridge VSI with the same input voltage. The block representation of PV with grid synchronization is illustrated in Fig 7.
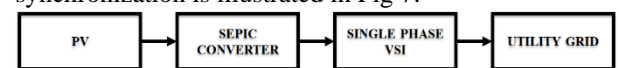

Fig. 7. Diagrammatic illustration of PV with grid-synchronization

The power quality issues like swell, sag, etc. occurs while synchronizing the 1Φ VSI with the grid, the above mentioned problems are overcome by using a filter which synchronizes the voltage into a sinusoidal form and so harmonics are minimized. The operating states of full bridge VSI are, the output voltage $+V_s$ is obtained by turning ON the switches S_1 and S_2, whereas the output voltage $-V_s$ is obtained by turning ON the

switches S_3 and S_4. The compensation of active and reactive power takes place by means of PI controller, by this the gating sequence for the 1Φ VSI is generated by comparing P_{act} with P_{ref} and so the grid synchronization is achieved.

4 Results and Discussions

The 1Φ grid connected PV system with SEPIC converter is apparently analysed in this present work and the outcomes of the system have been keenly examined. By utilising a SEPIC converter, the PV system's output voltage is increased to its maximum potential, improving system performance. The PI-based sea lion and dragonfly algorithm, in which PI parameters are tweaked, maintains the stability of the DC-link voltage. Table 1 presents the technical details of the PV module and SEPIC converter.

Table. 1. Specifications- PV module and SEPIC converter

| Components	Specifications
Total No. of modules	10
No. of series cells	36
Area of each cell	$125mm \times 31.25mm$
Operating Voltage	$16.8\ V$
Maximum Voltage	$1000\ V\ DC$
Operating Current	$5.8\ A$
Rating of Temperature	$-40\ to + 85℃$
Converter Ratings	
Input voltage, V_{PV}	$0\ to\ 48\ V\ DC$
Input current, I_i	$25\ A\ (Max)$
Capacitances, C_1, C_2	$20\ \mu F$
Inductances, L_1, L_2	$7\ mH$
Output current, I_o	$5\ A$
Operating frequency, f	$10\ KHz$
Output Power, P_o	$700\ W$
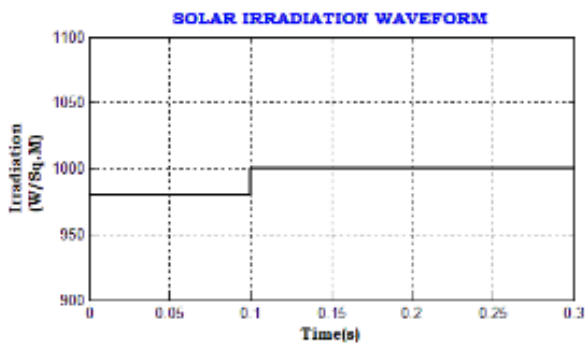
Fig. 8. Solar irradiation waveform

Solar irradiation waveform is illustrated in Fig 8. The solar irradiance varies throughout the day due to change in temperature. It can be seen from the waveform above that the sun irradiation level at 0.1 seconds ranges from $980\ W/m^2\ to\ 1000\ W/m^2$.
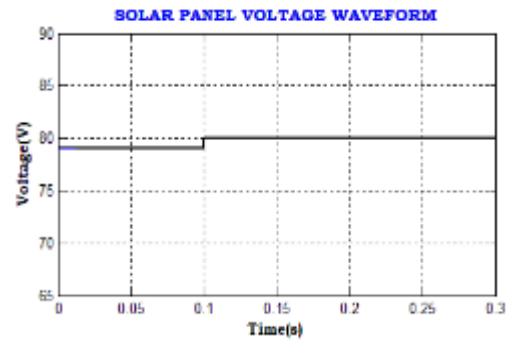
(a)
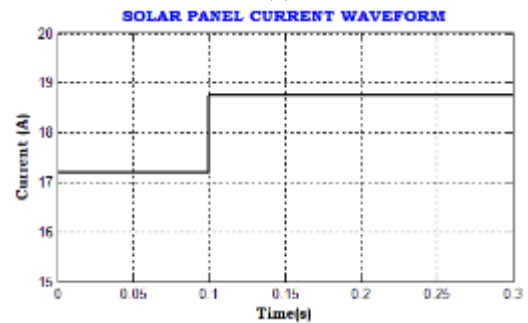
(b)

Fig. 9. (a) PV module voltage waveform (b) PV module current waveform

PV array's voltage and current waveform is illustrated in Fig 9 (a) & (b). Due to solar irradiation, the PV panel provides low DC voltage. From the Fig 9 (a) it is clearly revealed that, the output voltage of PV module ranges from $78\ V\ to\ 80\ V$ at the time period of $0.1\ s$ and from the Fig 9 (b) it is clearly revealed that, PV module output current fluctuates between $17.2\ A$ and $18.8\ A$ for 0.1 s.
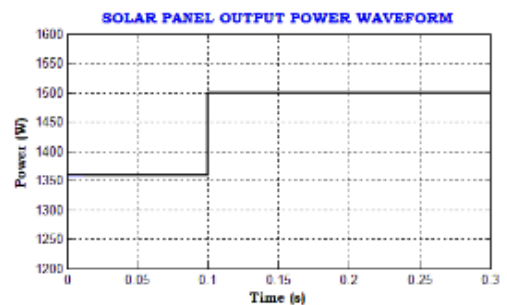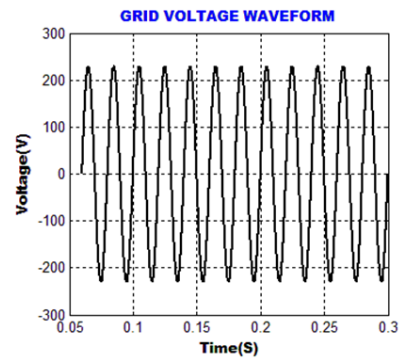
Fig. 10. PV array output power waveform

Fig. 10 shows the output power waveform of a PV array. It is evident from the above waveform that a PV module's output power at 0.1 seconds ranges from 1360 W to 1500 W.
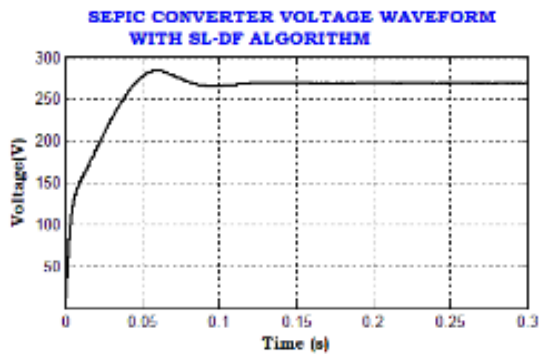

Fig. 11. SEPIC converter voltage waveform with SL-DF algorithm

Fig. 11 shows the SEPIC converter voltage waveform with the SL-DF algorithm. Low DC voltage from the PV output is increased using a SEPIC converter, and the output voltage of the SEPIC is DC-link voltage, which has been preserved using a hybrid sea lion and dragonfly algorithm. From the above waveform it is noted that, after time period of $0.11\ s$ DC-link voltage retains as constant.

The output of the SEPIC converter is sent into the PI controller-controlled VSI. Before being introduced into the grid, the VSI output has been filtered to remove distortions. The output voltage and current waveform produced by the grid are shown in Fig. 12.
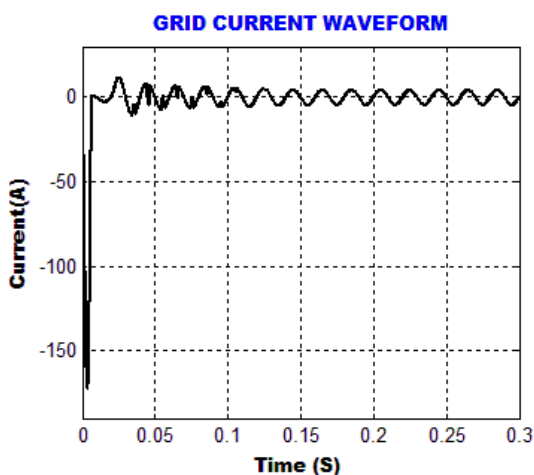

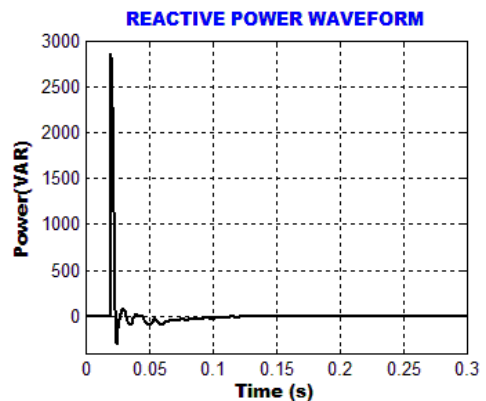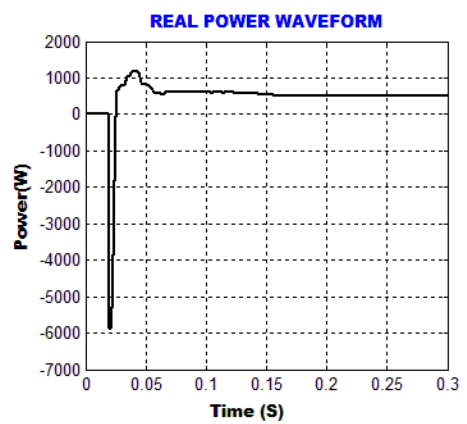**Fig. 12.** Generated output voltage and current waveform of grid

Fig. 13. Graphical representation of real and reactive power

The output of the VSI is regulated by the PI controller which supplies appropriate sinusoidal signal to the grid through the PWM generator. As shown in Fig 13, the real power rises initially and then reaches 500W whereas the reactive power drops to zero. According to Fig 14, the source current THD of the proposed system is significantly less and it is registered as 3.2%.
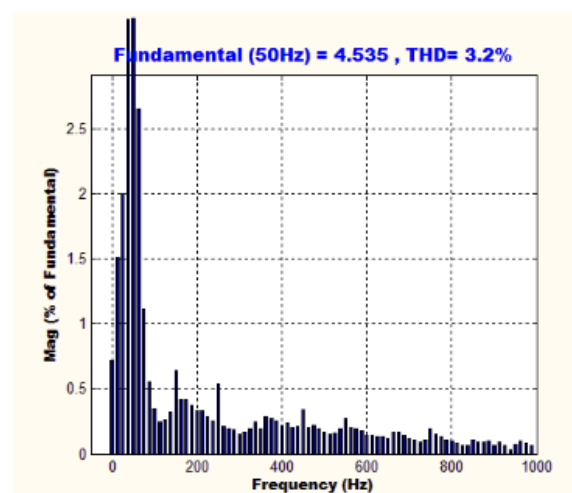

Fig. 14. THD waveform

Once the voltage gains of several converters have been analogized, it is evident that the SEPIC converter has the largest voltage gain ratio when compared to other

common converters like the CUK and Boost converter. While the voltage gain ratios of the CUK and Boost converters are reported as 1:2 and 1:1.5, respectively, the voltage gain ratio of the SEPIC converter is mentioned as 1:8. Fig 15 shows the voltage gain ratio comparison chart of different converters.
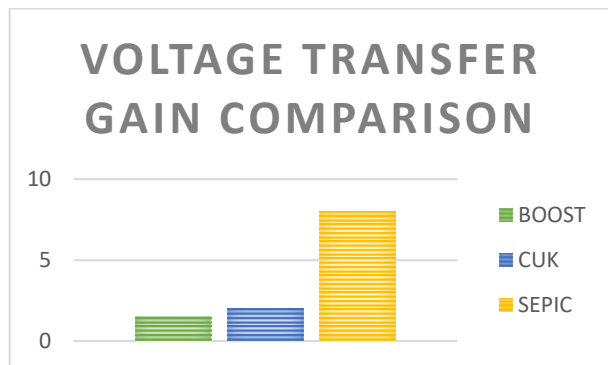

Fig. 15. Voltage gain ratio comparison chart

5 CONCLUSION

The present study has delineated implementation of PI based sea lion and dragonfly algorithm for grid connected PV system with SEPIC converter. The environmental circumstances have caused certain fluctuations in the PV output, which have been improvised by utilizing the proposed SEPIC converter. The DC-link voltage has been retained as stable through the implementation of PI based sea lion and dragonfly algorithm, which aids in tuning the parameters of PI. The output voltage of converter is then fed into grid through a 1Φ VSI, through which the DC link voltage is transformed as AC. By analogizing the P_{act} with P_{ref}, the gating pulses are produced and fed to the VSI with the aid of PI controller, through which the grid synchronization is accomplished. The whole control process has been validated through the MATLAB Simulink.

REFERENCES

[1].   N. Kumar, B. Singh and B. K. Panigrahi, "Framework of Gradient Descent Least Squares Regression-Based NN Structure for Power Quality Improvement in PV-Integrated Low-Voltage Weak Grid System," in IEEE Transactions on Industrial Electronics, Vol. 66, No. 12, pp. 9724-9733, 2019, doi: 10.1109/TIE.2018.2886765.

[2].   K. Sarita, S. Kumar, A. S. S. Vardhan, R. M. Elavarasan, R. K. Saket, G. M. Shafiullah, E. Hossain, "Power Enhancement With Grid Stabilization of Renewable Energy-Based Generation System Using UPQC-FLC-EVA Technique", IEEE Access, Vol. 8, pp. 207443 – 207464, 2020.

[3].   F. U. Nazir, N. Kumar, B. C. Pal, B. Singh and B. K. Panigrahi, "Enhanced SOGI Controller for Weak Grid Integrated Solar PV System," in IEEE Transactions on Energy Conversion, Vol. 35, No. 3, pp. 1208-1217,doi:10.1109/TEC.2020.2990866, 2020.

[4].   S. Pradhan, I. Hussain, B. Singh and B. K. Panigrahi, "Performance Improvement of Grid-Integrated Solar PV System Using DNLMS Control Algorithm", IEEE Transactions on Industry Applications, Vol. 55. No.1, pp. 78-91, 2019.

[5].   V. Karthikeyan, S. Kumaravel and G. Gurukumar, "High Step-Up Gain DC–DC Converter with Switched Capacitor and Regenerative Boost Configuration for Solar PV Applications", IEEE Transactions on Circuits and Systems II: Express Briefs, Vol. 66, No. 12, pp 2022 – 2026, 2019.

[6].   F. M. Alhuwaishel, A. K. Allehyani, Sinan A. S. Al-Obaidi and P. N. Enjeti, "A Medium-Voltage DC-Collection Grid for Large-Scale PV Power Plants With Interleaved Modular Multilevel Converter", IEEE Journal of Emerging and Selected Topics in Power Electronics, Vol. 8, No. 4, pp. 3434 – 3443, 2020.

[7].   M. W. Ahmad, N. B. Y. Gorla, H. Malik and S. K. Panda, "A Fault Diagnosis and Postfault Reconfiguration Scheme for Interleaved Boost Converter in PV-Based System," in IEEE Transactions on Power Electronics, Vol. 36, No. 4, pp. 3769-3780, 2021, doi: 10.1109/TPEL.2020.3018540.

[8].   Ghazaly, N. M. . (2022). Data Catalogue Approaches, Implementation and Adoption: A Study of Purpose of Data Catalogue. International Journal on Future Revolution in Computer Science &Amp; Communication Engineering, 8(1), 01–04. https://doi.org/10.17762/ijfrcsce.v8i1.2063

[9].   D. Yamaguchi and H. Fujita, "A New PV Converter for a High-Leg Delta Transformer Using Cooperative Control of Boost Converters and Inverters", IEEE Transactions on Power Electronics, Vol. 33, No. 11, pp. 9542 – 9550, 2018.

[10].   Q. Huang, A. Q. Huang, R. Yu, P. Liu and W. Yu, 2019, "High-Efficiency and High-Density Single-Phase Dual-Mode Cascaded Buck–Boost Multilevel Transformerless PV Inverter With GaN AC Switches", IEEE Transactions on Power Electronics, Vol. 34, No. 8, pp. 7474 – 7488.

[11].   Ahmed Cherif Megri, Sameer Hamoush, Ismail Zayd Megri, Yao Yu. (2021). Advanced Manufacturing Online STEM Education Pipeline for Early-College and High School Students. Journal of Online Engineering Education, 12(2), 01–06. Retrieved from http://onlineengineeringeducation.com/index.php/joee/article/view/47

[12].   K. Nathan, S. Ghosh, Y. Siwakoti and T. Long, "A New DC–DC Converter for Photovoltaic Systems: Coupled-Inductors Combined Cuk-SEPIC Converter", IEEE Transactions on Energy Conversion, Vol. 34, No. 1, pp. 191 – 201, 2019.

[13].   J. C. d. S. de Morais, J. L. d. S. de Morais and R. Gules, "Photovoltaic AC Module Based on a Cuk Converter With a Switched-Inductor Structure," in IEEE Transactions on Industrial Electronics, Vol. 66, No. 5, pp. 3881-3890, 2019, doi: 10.1109/TIE.2018.2856202.

[14].   Hermina, J. ., Karpagam, N. S. ., Deepika, P. ., Jeslet, D. S. ., & Komarasamy, D. (2022). A Novel Approach to Detect Social Distancing Among People in College Campus. International Journal of Intelligent Systems

and Applications in Engineering, 10(2), 153–158. Retrieved from https://ijisae.org/index.php/IJISAE/article/view/1823

[15]. M. A. Ghasemi, H. M. Foroushani and F. Blaabjerg, "Marginal Power-Based Maximum Power Point Tracking Control of Photovoltaic System Under Partially Shaded Condition," in IEEE Transactions on Power Electronics, Vol. 35, No. 6, pp. 5860-5872, 2020, doi: 10.1109/TPEL.2019.2952972.

[16]. M. Kermadi, Z. Salam, J. Ahmed and E. M. Berkouk, "A High-Performance Global Maximum Power Point Tracker of PV System for Rapidly Changing Partial Shading Conditions," in IEEE Transactions on Industrial Electronics, Vol. 68, No. 3, pp. 2236-2245, 2021, doi: 10.1109/TIE.2020.2972456.

[17]. N. Ullah, F. Nisar and A. A. Alahmadi, "Closed Loop Control of Photo Voltaic Emulator Using Fractional Calculus," in IEEE Access, Vol. 8, pp. 28880-28887, 2020, doi:10.1109/ACCESS.2020.2971676.

[18]. R. Errouissi and A. Al-Durra, "Design of PI Controller Together With Active Damping for Grid-Tied LCL-Filter Systems Using Disturbance-Observer-Based Control Approach," in IEEE Transactions on Industry Applications, Vol. 54, No. 4, pp. 3820-3831, 2018, doi: 10.1109/TIA.2018.2823258.

[19]. M. A. Hannan, J. A. Ali, A. Mohamed, U. A. U. Amirulddin, N. M. L. Tan and M. N. Uddin, "Quantum-Behaved Lightning Search Algorithm to Improve Indirect Field-Oriented Fuzzy-PI Control for IM Drive," in IEEE Transactions on Industry Applications, Vol. 54, No. 4, pp. 3793-3805, 2018, doi: 10.1109/TIA.2018.2821644.

[20]. Goar, . V. K. ., and N. S. . Yadav. "Business Decision Making by Big Data Analytics". International Journal on Recent and Innovation Trends in Computing and Communication, vol. 10, no. 5, May 2022, pp. 22-35, doi:10.17762/ijritcc.v10i5.5550.

[21]. S. Yousaf, A. Mughees, M. G. Khan, A. A. Amin and M. Adnan, "A Comparative Analysis of Various Controller Techniques for Optimal Control of Smart Nano-Grid Using GA and PSO Algorithms," in IEEE Access, Vol. 8, pp. 205696-205711, 2020, doi: 10.1109/ACCESS.2020.3038021.

[22]. M. U. Jan, A. Xin, M. A. Abdelbaky, H. U. Rehman and S. Iqbal, "Adaptive and Fuzzy PI Controllers Design for Frequency Regulation of Isolated Microgrid Integrated With Electric Vehicles," in IEEE Access, Vol. 8, pp. 87621-87632, 2020, doi: 10.1109/ACCESS.2020.2993178.

[23]. M. H. Qais, H. M. Hasanien and S. Alghuwainem, "A Grey Wolf Optimizer for Optimum Parameters of Multiple PI Controllers of a Grid-Connected PMSG Driven by Variable Speed Wind Turbine," in IEEE Access, Vol. 6, pp. 44120-44128, 2018, doi: 10.1109/ACCESS.2018.2864303.

[24]. K. Guo, L. Cui, M. Mao, L. Zhou and Q. Zhang, "An Improved Gray Wolf Optimizer MPPT Algorithm for PV System With BFBIC Converter Under Partial Shading," in IEEE Access, vol. 8, pp. 103476-103490, 2020, doi: 10.1109/ACCESS.2020.2999311.

[25]. H. Watanabe, T. Sakuraba, K. Furukawa, K. Kusaka and J. -i. Itoh, "Development of DC to Single-Phase AC Voltage Source Inverter With Active Power Decoupling Based on Flying Capacitor DC/DC Converter," in IEEE Transactions on Power Electronics, Vol. 33, No. 6, pp. 4992-5004, 2018, doi: 10.1109/TPEL.2017.2727063.